



TITLE:

# Vision-based uncut crop edge detection for automated guidance of head-feeding combine

AUTHOR(S):

Cho, Wonjae; Iida, Michihisa; Suguri, Masahiko; Masuda, Ryohei; Kurita, Hiroki

---

CITATION:

Cho, Wonjae ...[et al]. Vision-based uncut crop edge detection for automated guidance of head-feeding combine. Engineering in Agriculture, Environment and Food 2014, 7(2): 97-102

ISSUE DATE:

2014-04

URL:

<http://hdl.handle.net/2433/189414>

RIGHT:

© 2014 Asian Agricultural and Biological Engineering Association. Published by Elsevier B.V.; この論文は出版社版ではありません。引用の際には出版社版をご確認ご利用ください。 ; This is not the published version. Please cite only the published version.

# Vision-based Uncut Crop Edge Detection for Automated Guidance of Head-Feeding Combine

Wonjae CHO<sup>\*1</sup>, Michihisa IIDA<sup>\*2</sup>, Masahiko SUGURI<sup>\*3</sup>,  
Ryohei MASUDA<sup>\*3</sup>, Hiroki KURITA<sup>\*3</sup>

## Abstract

This study proposes a vision-based uncut crop edge detection method to be utilized as a part of an automated guidance system for a head-feeding combine harvester, which is widely used in Japan for the harvesting of rice and wheat. The proposed method removes the perspective effects of the acquired images by inverse perspective mapping and recovers the crop rows to their actual parallel states. Then, the uncut crop edges are detected by applying color transformation and the edge detection method. The proposed method has shown outstanding detection performance on the images acquired under various conditions of the paddy field with an average accuracy of 97% and a processing speed of 33 ms per frame.

[Keywords] Head-feeding combine harvester, Uncut crop edge detection, Inverse perspective mapping, Color transformation

## I Introduction

Operation of a harvester in the field is demanding for the operator because the work is time-consuming and to deteriorates the health of the operator owing to, dust particles as well as the noise and vibrations of the harvesting machine. Moreover, the steering operation requires the operator to possess a high level of proficiency to compensate for the inefficiencies of inaccurate steering, which could result in incompletely harvested areas or re-harvesting of the areas. To address such issues, automated guidance systems can steer automatically by the edges of uncut crops to fully complete the demanding tasks.

Because the automated guidance system provides an optimal steering path after considering the machinery environment, it reduces operator fatigue and improves both safety and productivity of the operations. The automated guidance system consists of two parts including an autonomous system and an operator-assisted system (Kise, *et al.*, 2005). The autonomous system replaces the role of the operator in the field and performs all operations, completing the harvesting task automatically. The operator-assisted system merely assists the operator and guides the machinery toward the desired path. Although the two systems differ in functionality, both perform path planning by navigation

sensors mounted on the machinery. The automated guidance system of the harvesting machine repeats the following process until harvesting is complete: The current position of the machinery is first estimated in real-time, and the course direction is determined by the extraction of the uncut crop edges. Next, an optimal path with minimum time consumption that does not damage the crops is planned for the steering. Finally, the machinery is steered along the desired path. As previously described, because the automated guidance system performs path planning and accurate steering on the basis of the uncut crop edges extracted by the use of navigation sensors mounted on the machinery, precise extraction of the edges is critical to the system performance.

In recent years, various sensor methodologies have been proposed or developed for automated guidance systems of harvesting machines. Researchers from the National Agricultural Research Center in Japan and Mitsubishi Farm Machinery Co., Ltd. have developed an automatic travelling control system that performs straight-forward traveling movement by detecting uncut crops and incorporating a 90° turn by using the gyroscope mounted on the combine body when the harvester reaches the end of crop row. This action is performed by utilizing the contact sensor mounted on the header's divider of the head-feeding combine harvester (Sato, *et*

\*1 JSAM Student Member, Graduate School of Agriculture, Kyoto University, Kitashirakawa Oiwake-cho, Sakyo-ku, Kyoto, 606-8502, Japan; cho@elam.kais.kyoto-u.ac.jp

\*2 JSAM Member, Corresponding author, Graduate School of Agriculture, Kyoto University, Kitashirakawa Oiwake-cho, Sakyo-ku, Kyoto, 606-8502, Japan; iida@elam.kais.kyoto-u.ac.jp

\*3 JSAM Member, Graduate School of Agriculture, Kyoto University, Kitashirakawa Oiwake-cho, Sakyo-ku, Kyoto, 606-8502, Japan

*al.*, 1996). Researchers from Carnegie Mellon University and the National Aeronautic and Space Administration (NASA) developed an automated guidance system that employs a color camera to extract the uncut crop edges to perform the automatic guiding task. This system was tested on a New Holland hay windrower and has successfully performed a harvesting task in an alfalfa field (Ollis and Stentz, 1997). Researchers from Cemagref Institute in France proposed an automatic guidance method for agricultural vehicles in either a structured environment, such as a windrow harvester, or an iterative structured environment, such as a combine harvester, by implementing a 1D scanning laser range finder (Chateau, *et al.*, 2000). Benson, *et al.* (2003) developed and demonstrated a machine-vision-based guidance system for small-grain harvesters with the use of a monochrome camera mounted on the machinery cab. Rovira-Más, *et al.* (2007) developed an autonomous guidance system that extracts the edges of uncut crops on the basis of 3D information obtained from stereo vision.

This study proposes a vision-based uncut crop edge detection method for an automated guidance system that can be utilized for a head-feeding combine harvester, which is widely used in Japan for harvesting rice and wheat. The proposed method detected the uncut crop edges at a processing speed of 33 ms per frame in the paddy field under the conditions of various noise elements, shadows casted by irregular crop distribution and the driving direction of the combine harvester as well as dust particles generated by harvesting. Moreover, unlike previous researchers who detect uncut crop edges without removing the perspective effect existing on the images acquired from a single vision sensor (Ollis and Stentz, 1997; Benson, *et al.*, 2003), the present study identifies the relative lateral distance of the uncut crop edge from the center of origin of the vision sensor because this way it extracts the uncut crop edges by applying the inverse perspective mapping (IPM) algorithm to an image that uses the extrinsic and intrinsic parameters of the single-vision sensor. This process removes the perspective effect existing within the images and converts the location information of the image plane to that of the world coordinate system.

## II Materials and Methods

### 1. Experimental setup

A VY446LM model head-feeding combine harvester (Mitsubishi Agricultural Machinery Co., Ltd., Japan) was used for experiments in this study. This harvester can

simultaneously harvest four rows of rice in a paddy field. The harvester driven by a human operator harvested rice at a speed of 0.8 m/s. The Microsoft LifeCam Studio vision sensor (Microsoft Co., Ltd.), which supports the USB 2.0 interface, was used for uncut crop edge detection. The vision sensor operates within a temperature range of 0 °C to 40 °C and a relative humidity range of 5% to 80%. A complementary metal-oxide semiconductor image sensor was used, which has a field of view of 75°. The sensor captures 10 frames of color images in 640 pixel (horizontal) by 480 pixel (vertical) resolution per second. As shown in Fig. 1, the camera is mounted on the frame located at the front of the cab of the head-feeding combine harvester. The center of the lens is located 1.5m vertically ( $h$ ) from the ground, with a tilt angle ( $\theta$ ) of 10°. A computer with Corei5 CPU 2.40 GHz and 4GB memory was used.

This study utilized the machine vision function of the integrated sensor control platform (ISCP) for combine harvesters, which is currently under development for the implementation of a vision-based guidance method. ISCP supports various types of navigation sensors such as machine vision, laser range finder, and global positioning system (GPS), which are used for the automated guidance system of the combine harvester. This platform can also express graphic user interface (GUI)-based real-time data. Moreover, the open-source platform can freely be modified and re-distributed without license restrictions. The proposed vision-based guidance method was developed by using Visual C# language, and the open source computer vision (OpenCV) library was utilized for image processing.

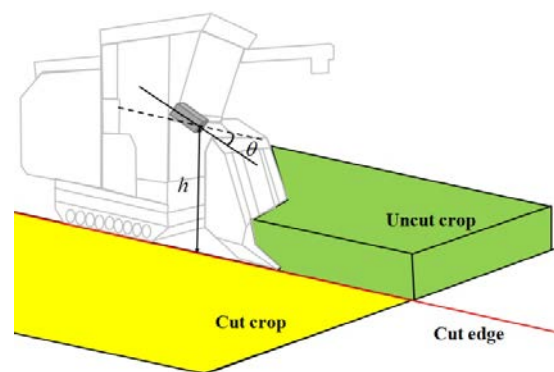


Fig. 1. Coordinate system of the camera mounted on the combine harvester.

### 2. Inverse perspective mapping

In the paddy fields of Japan, rice plants are evenly planted at approximately 0.3 m in the inter-row ( $d_r$ ) and approximately 0.15 m in the intra-row ( $d_c$ ) in a parallel

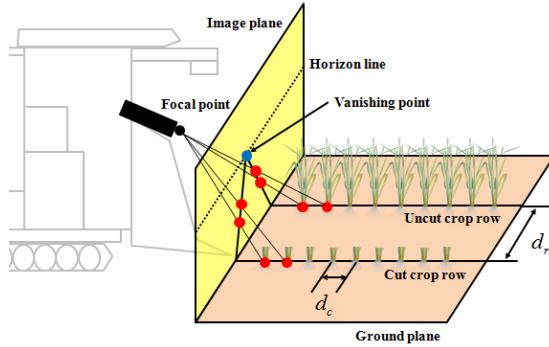


Fig. 2. Geometry of the central projective model.

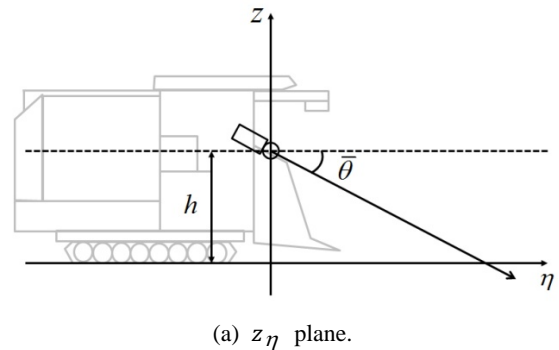
For the purpose of this study, IPM was utilized to remove the perspective effect and restore the crop rows to their original parallel state. IPM is a technique that geometrically transforms an image by constructing a new image on inverse 2D planar by projecting each of the pixels of a 3D object in 2D perspective view and remapping them to new positions (Bertozzi and Broggi, 1998). IPM removes the perspective effect by the use of intrinsic (angular aperture and resolution) and extrinsic (pitch angle, yaw angle, and height above ground) parameters of the camera. It also has the ability to calculate lateral distances between the crop rows from the point of origin of the camera because it converts the position information of the image plane to that of the world coordinate system. IPM, in the mathematical sense, is a transformation of a 3D Euclidean space,  $W = \{(x, y, z)\} \in E^3$  (world space), into a 2D Euclidean space,  $I = \{(u, v)\} \in E^2$  (image space). Whereas Space  $I$  corresponds to the image acquired, the remapped image is defined under the flatness assumption on the  $xy$  plane of Space  $W$ , namely the  $S \triangleq \{(x, y, 0) \in W\}$  surface. Fig. 3 shows the extrinsic parameters of the camera mounted on the combine harvester. Parameters  $\bar{\gamma}$ ,  $\bar{\theta}$ , and  $h$  denote the yaw angle, pitch angle, and the height of the camera from the ground, respectively, and  $l$  and  $d$  represent the longitudinal and transverse distances of the camera to the center of origin on the  $xy$  plane. The intrinsic parameters are expressed as the angular aperture  $2\alpha$  and resolution  $m \times n$ . By using the extrinsic and intrinsic parameters, the mapping function from Space  $I$  to Space  $S$  can be defined as in Eq. (1): ( $f: I \rightarrow S$ ).

$$\begin{aligned} x(u, v) &= h \times \cot[(\bar{\theta} - \alpha) + u \frac{2\alpha}{n-1}] \\ &\quad \times \cos[(\bar{\gamma} - \alpha) + v \frac{2\alpha}{m-1}] + l \\ y(u, v) &= h \times \cot[(\bar{\theta} - \alpha) + u \frac{2\alpha}{n-1}] \\ &\quad \times \sin[(\bar{\gamma} - \alpha) + v \frac{2\alpha}{m-1}] + d \\ z(u, v) &= 0 \end{aligned} \quad (1)$$

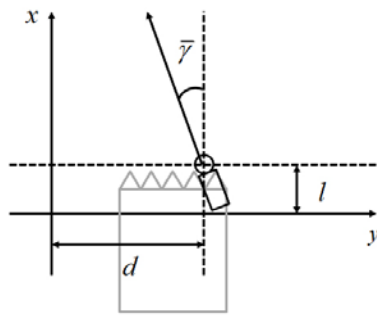
Moreover, Eq. (2) defines the projection transformation used to remove the perspective effect, which recovers the texture of the  $S$  surface (the  $z = 0$  plane in Space  $W$ ).

$$\begin{aligned} u(x, y, 0) &= \frac{\arctan\left\{\frac{h \sin\left[\arctan\left(\frac{y-d}{x-l}\right)\right]}{y-d}\right\} - (\bar{\theta} - \alpha)}{\frac{2\alpha}{n-1}} \\ v(x, y, 0) &= \frac{\arctan\left[\frac{y-d}{x-l}\right] - (\bar{\gamma} - \alpha)}{\frac{2\alpha}{m-1}} \end{aligned} \quad (2)$$

Each pixel scanned from the coordinates  $(x, y, 0) \in W$ , which forms the remapped image, is assigned the value of its corresponding pixel in the coordinates  $(u(x, y, 0), v(x, y, 0)) \in I$ . Once these two equations are applied, the window of interest from the input image can be projected onto the ground plane. Fig. 4 shows the original image acquired from the camera and the image transformed by the IPM algorithm. The original image ( $640 \times 480$  pixels) is shown in Fig. 4(a), with the region of interest (ROI;  $640 \times 400$  pixels) shown in the square (red); the transformed IPM image ( $320 \times 240$  pixels) is shown in Fig. 4(b). As indicated in the figure, the IPM image shows the crop rows in fixed width intervals as vertical, straight lines in a parallel configuration.



(a)  $z\eta$  plane.

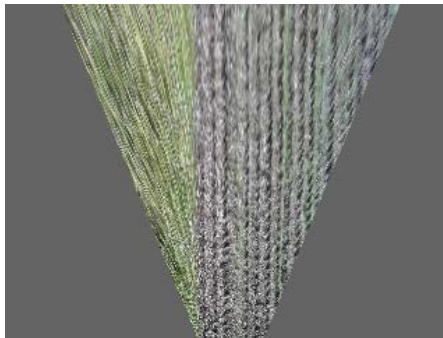


(b)  $xy$  plane.

Fig. 3. Extrinsic parameters of the camera.



(a) Input image, the region of interest marked off.



(b) Inverse perspective mapping (IPM) view.

Fig. 4. Original image and the converted inverse perspective mapping (IPM) image.

### 3. Color space transformation

The IPM images, transformed in the RGB color space, contain the surrounding information about shadows, dust particles floating in air, and any potential noise that might have been generated as the result of radical brightness changes in the surroundings. Therefore, prior to applying the uncut crop edge detection algorithm, a robust segmentation method is required to filter out the noise in the images and extract the uncut crop areas. Under this backdrop, color indices have been developed that can distinguish crops from other image elements (Woebbecke, *et al.*, 1995; Meyer, *et al.*, 1998; Kataoka, *et al.*, 2003; Neto, 2004; Hague, *et al.*, 2006). By the

image transformation into these indices, the spectral differences between plants and the rest of the image areas are contrasted. In the present study, the excess green minus excess blue index (ExGB), based on the visible spectral indices proposed by early researchers, has been applied to the images to perform segmentations. ExGB is defined as

$$r = \frac{R}{R+G+B}, g = \frac{G}{R+G+B}, b = \frac{B}{R+G+B} \quad (3)$$

Excess green:  $\text{ExG} = 2g - r - b$

Excess blue:  $\text{ExB} = 1.4b - g$

Excess green minus excess blue:  $\text{ExGB} = \text{ExG} - \text{ExB}$

where  $R$ ,  $G$ , and  $B$  are normalized RGB coordinates that range from 0 to 1. They are obtained from Eq.(4):

$$R = \frac{R}{R_{\max}}, G = \frac{G}{G_{\max}}, B = \frac{B}{B_{\max}} \quad (4)$$

where  $R_{\max} = G_{\max} = B_{\max} = 255$  (for 24-bit color images). Thus, on the basis of normalized RGB coordinates, these indices become insensitive to the changes that arise from ambient light conditions as well as to the differences in the angles to target surfaces. Fig. 5 shows the results of the uncut crop segmentation by applying the ExGB method to transformed IPM images. In the grayscale-converted ExGB images, it is likely that the higher pixel values represent uncut crop areas and that the lower values indicate harvested crops or image noise.

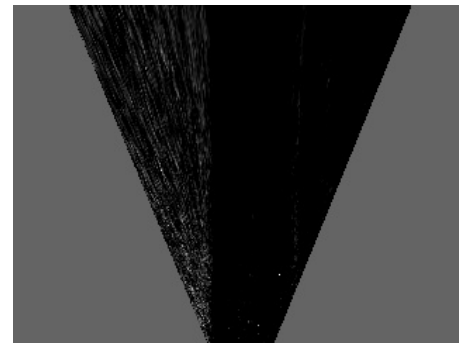


Fig. 5. Excess green minus excess blue index (ExGB) image.

### 4. Uncut crop edge detection

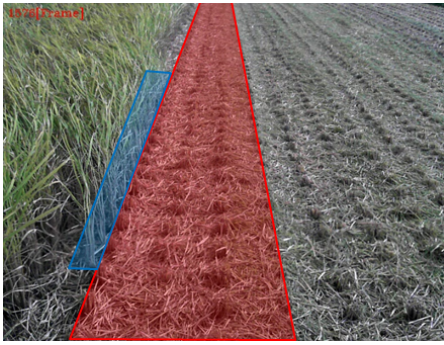
The precise steering of a harvesting machine along uncut crop edges would leave no uncut crops in the rows from the previous harvesting path as shown in Fig. 6(a). However, if the steering is not precise, there would be uncut remains in the crop rows from the harvesting path, as shown in Fig. 6(b). In such cases, unless the next harvesting path is determined by detection of the uncut crop edges of the previous harvest path, re-harvesting is



- 1 required after the completion of the overall harvesting,
- 2 which would decrease the harvest efficiency.



(a) No uncut crops after precise steering



(b) Remaining uncut crops after imprecise steering.

Fig. 6. Uncut crop remainders in planned harvest paths due to differences in steering performance.

Therefore, in this study, the outer-most boundary point of the uncut crop area is detected from the image for configuring the uncut crop edge. In this process, two techniques are applied. ExGB images are first scanned left to right for each row. The average gray level for each column is then calculated and stored in an array of  $S = \{p_i | i = 1, \dots, n\}$ ;  $n$  is number of columns. Fig. 7 shows the average distribution of the gray level for the pixels of each column; the abscissa is the number of columns for the grayscale image, and the vertical axis is the average pixel gray level for each column.

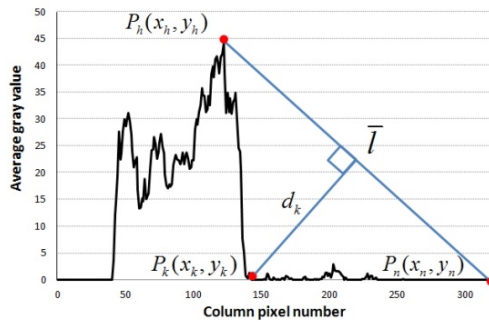
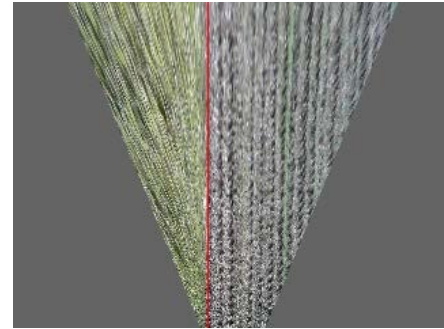


Fig. 7. Average distribution of the gray level value per column pixels.

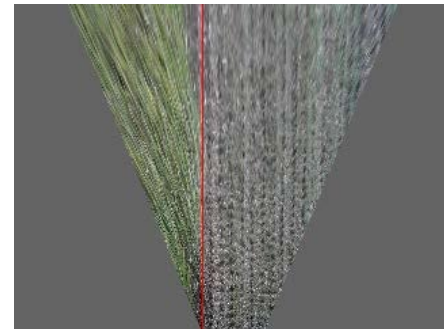
- 25 Because harvesting was performed counter-clockwise
- 26 in the course of this study, the uncut crop area is located
- 27 on the left side of the uncut crop edge in the acquired
- 28 image, and the harvested area appears on the right.
- 29 Leveraging on such characteristics, the line segment ( $\bar{l}$ ),
- 30 the connection between the maximum value of the
- 31 average gray level ( $p_h$ ) and the end point ( $p_n$ ) within
- 32 dataset  $S$  is calculated. Then, the point ( $p_k$ ), in which
- 33 the distance of the line perpendicular ( $d_k$ ) to segment  $\bar{l}$
- 34 from data set  $V = \{p_i | i = h, \dots, n\}$  reaches the
- 35 maximum, is calculated by Eq. (5) (Kimberling, 1998) .

$$d_k = \frac{|(x_n - x_h)(y_h - y_k) - (x_h - x_k)(y_n - y_h)|}{\sqrt{(x_n - x_h)^2 + (y_n - y_h)^2}} \quad (5)$$

- 37 Because the  $x$  value of the calculated  $p_k$  represents
- 38 the outer-most boundary point of the uncut area, the
- 39 uncut and harvested areas can be distinguished from the
- 40 image on the basis of this value. Fig. 8 shows the results
- 41 of the application of the proposed methods to Fig. 6(a)
- 42 and Fig. 6(b). Because the proposed detection method
- 43 defines the uncut crop edges on the basis of the
- 44 outer-most boundary point of the uncut area, it can
- 45 ideally and accurately detect the edges from that shown
- 46 in Fig. 6(a), in which the previous harvest is precisely
- 47 completed, and for that shown in Fig. 6(b), in which
- 48 uncut remainders exist in the crops rows of the previous
- 49 harvest.



(a) Edge detection in Fig. 6(a).



(b) Edge detection in Fig. 6(b).

Fig. 8. Successful uncut crop edge detection.

### III Results and Discussion

For the evaluation of the outdoor performance of the proposed method, actual rice harvesting images from a rice paddy field in Nantan City, Kyoto Prefecture, Japan, were acquired under sunny conditions. *Oryza sativa L.* (cv. *Kinu-hikari*) was the crop harvested for the experiment. As a human operator steered the combine harvester, the scenes were stored and saved in video format (Audio Video Interleave). Because the combine harvester travelled counter-clockwise during the harvesting period, as shown in Fig. 9, the noise levels in the acquired images differ as the light conditions changed depending on the movement direction.

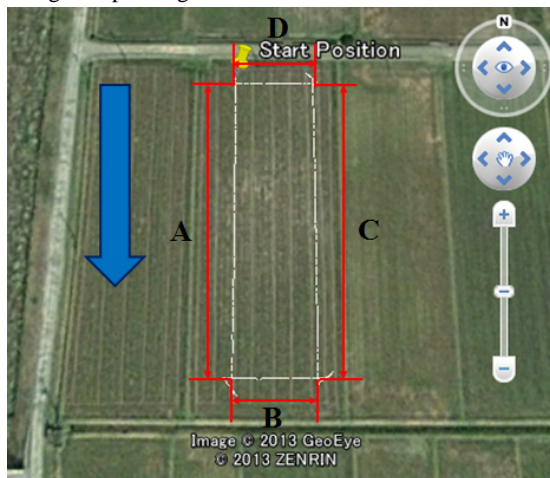


Fig. 9. Travelling path of the combine harvester obtained from Google Maps.

For easier comparison of the results, all of the acquired images were categorized into four datasets, according to the directions of the harvester movement, as shown in Table 1. The success of the uncut crop edge detection was determined through human eye perception. The video results can be accessed at <http://youtu.be/wJ5u850aQII>.

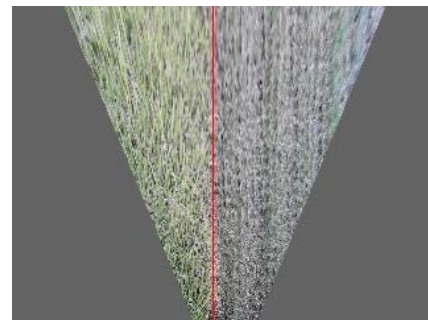
Table 1 Results determined by the proposed method.

| Dataset | Movement direction | Frames | Success Rate [%] |
|---------|--------------------|--------|------------------|
| A       | South              | 950    | 100              |
| B       | East               | 300    | 100              |
| C       | North              | 950    | 94               |
| D       | West               | 300    | 100              |

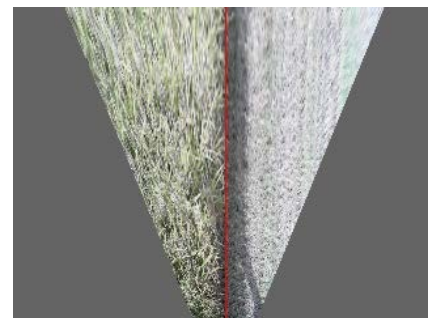
The evaluation results show that the proposed method is effective in detecting the uncut crop edges from the images under various conditions. The average detection accuracy of the uncut crop edge by the proposed method was 97% at an average processing speed of 33 ms per

frame. The evaluation results show that the proposed method can detect the edges of the uncut crops with relatively high accuracy regardless of to the movement direction of the combine harvest or the noise from the surrounding conditions, as shown in Fig. 10.

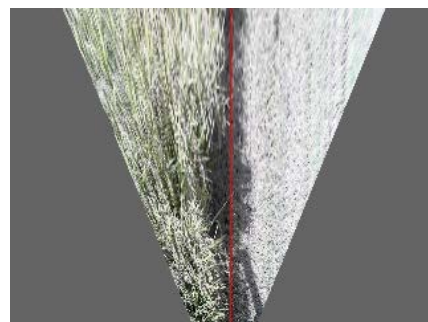
However, as shown in Fig. 11(a), in which the combine harvester was heading north (dataset C), the uncut crop detection was not successful owing to the combination of image information including shadows cast by the machine and the uncut crops and the random patterns of uncut crops left in the previous harvesting path. Of course, because uncut crop edges were successfully detected in Fig. 11(b), the image was consecutively acquired after Fig. 11(a), the detection can be corrected by adjusting the guidance path by steering. However, it is likely that the rapid steering of the combine harvester may cause uncut crops to remain in the rows of the previous harvest paths. Therefore, an algorithm to calibrate and adjust the failures in detecting uncut crop edges should be developed.



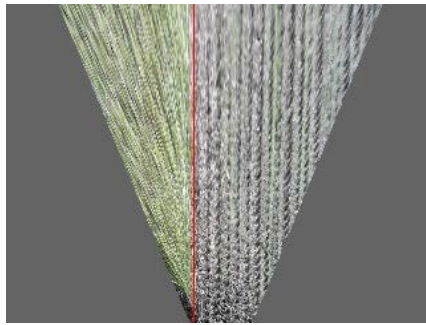
(a) Facing the sun.



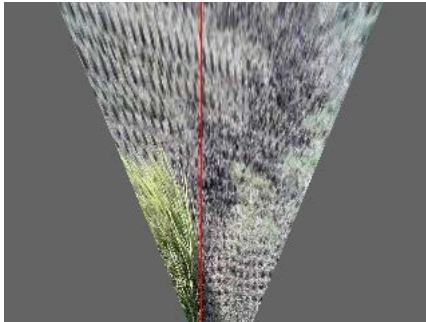
(b) Back to sun and shadow.



(c) Random uncut crop distribution.

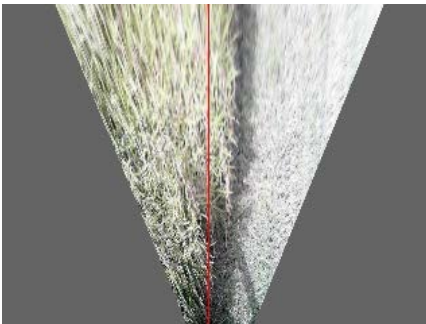


(d) Beginnig of harvest.

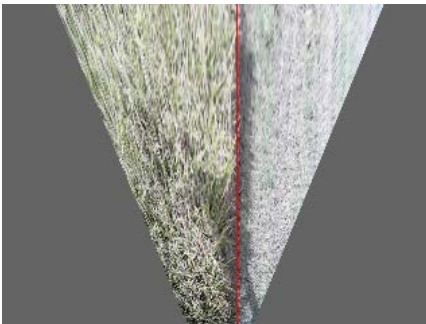


(e) End of harvest.

Fig. 10. Results of uncut crop edge detection under various experimental conditions.



(a) Before, unsuccessful detection of uncut crop edge.



(b) After, Successfully detection of uncut crop edge.

Fig. 11. Detection results in consecutively acquired images.

#### IV Summary and Conclusions

This study proposed a robust, efficient, and real-time method for the detection of uncut crop edges to be

utilized in paddy fields. The proposed method acquires top view images of the field, which are then filtered with ExGB and uncut edge detection algorithms. The tested method detected nearly all uncut crop edges, as shown in still images of the paddy field, and performed image processing at a speed of 33 ms per frame. However, its performance was poor under certain environmental conditions. Thus, a new algorithm to calibrate and adjust such failures in uncut crop edge detection should be developed. Moreover, future developments should consider methods for providing robust guidance by the use of vision sensors together with other navigation sensors, such as GPS or laser range finders.

#### References

- Benson, E. R., J. F. Reid and Q. Zhang. 2003. Machine vision-based guidance system for agricultural grain harvesters using cut-edge detection. *Biosystems Engineering* 86(4): 389-398.
- Bertozzi, M. and A. Broggi. 1998. GOLD: A parallel real-time stereo vision system for generic obstacle and lane detection. *IEEE Transactions on Image Processing* 7(1): 62-81.
- Chateau, T., C. Debain, F. Collange, L. Trassoudaine and J. Alizon. 2000. Automatic guidance of agricultural vehicles using a laser sensor. *Computers and Electronics in Agriculture* 28(3): 243-257.
- Hague, T., N. D. Tillett and H. Wheeler. 2006. Automated crop and weed monitoring in widely spaced cereals. *Precision Agriculture* 7(1): 21-32.
- Kataoka, T., T. Kaneko, H. Okamoto and S. Hata. 2003. Crop growth estimation system using machine vision. In *Proc. IEEE/ASME International Conference on Advanced Intelligent Mechatronics*, b1079-b1083.
- Kimberling, C. 1998. *Triangle centers and central triangles*. Utilitas Mathematica Publishing, Inc.
- Kise, M., Q. Zhang and F. Rovira Más. 2005. A stereovision-based crop row detection method for tractor-automated guidance. *Biosystems Engineering* 90(4): 357-367.
- Meyer, G. E., T. Mehta, M. F. Kocher, D. A. Mortensen and A. Samal. 1998. Textural imaging and discriminant analysis for distinguishing weeds for spot spraying. *Transactions of the ASAE* 41(4): 1189-1197.
- Neto, J. C. 2004. A combined statistical-soft computing approach for classification and mapping weed species in minimum-tillage systems. University of Nebraska, Lincoln, NE.
- Ollis, M. and A. Stentz. 1997. Vision-based perception for an automated harvester. In *Proc. IEEE/RSJ International*



- 1 Conference on Intelligent Robots and Systems, 1838-1844.
- 2 September.
- 3 Rovira-Más, F., S. Han, J. Wei and J. F. Reid. 2007.
- 4 Autonomous guidance of a corn harvester using stereo
- 5 vision. *Agricultural Engineering International: the CIGR*
- 6 *Ejournal* 9.
- 7 Sato, J., K. Shigeta and Y. Nagasaka. 1996. Automatic operation
- 8 of a combined harvester in a rice field. In *Proc.*
- 9 *IEEE/SICE/RSJ International Conference on Multisensor*
- 10 *Fusion and Integration for Intelligent Systems*, 86-92.
- 11 Washington, DC, 8-11 December.
- 12 Woebbecke, D. M., G. E. Meyer, K. Von Bargen and D. A.
- 13 Mortensen. 1995. Color indices for weed identification
- 14 under various soil, residue, and lighting conditions.
- 15 *Transactions of the ASAE* 38(1): 259-269.
- 16 (Received : X. January. 20XX, Accepted : X. February. 20XX)